LETTERS

Primary contribution to zebrafish heart regeneration by *gata4*$^+$ cardiomyocytes

Kazu Kikuchi[1,2], Jennifer E. Holdway[1,2], Andreas A. Werdich[4], Ryan M. Anderson[5], Yi Fang[1,2], Gregory F. Egnaczyk[1,2,3], Todd Evans[6], Calum A. MacRae[4], Didier Y. R. Stainier[5] & Kenneth D. Poss[1,2]

Recent studies indicate that mammals, including humans, maintain some capacity to renew cardiomyocytes throughout postnatal life[1,2]. Yet, there is little or no significant cardiac muscle regeneration after an injury such as acute myocardial infarction[3]. By contrast, zebrafish efficiently regenerate lost cardiac muscle, providing a model for understanding how natural heart regeneration may be blocked or enhanced[4,5]. In the absence of lineage-tracing technology applicable to adult zebrafish, the cellular origins of newly regenerated cardiac muscle have remained unclear. Using new genetic fate-mapping approaches, here we identify a population of cardiomyocytes that become activated after resection of the ventricular apex and contribute prominently to cardiac muscle regeneration. Through the use of a transgenic reporter strain, we found that cardiomyocytes throughout the subepicardial ventricular layer trigger expression of the embryonic cardiogenesis gene *gata4* within a week of trauma, before expression localizes to proliferating cardiomyocytes surrounding and within the injury site. Cre-recombinase-based lineage-tracing of cells expressing *gata4* before evident regeneration, or of cells expressing the contractile gene *cmlc2* before injury, each labelled most cardiac muscle in the ensuing regenerate. By optical voltage mapping of surface myocardium in whole ventricles, we found that electrical conduction is re-established between existing and regenerated cardiomyocytes between 2 and 4 weeks post-injury. After injury and prolonged fibroblast growth factor receptor inhibition to arrest cardiac regeneration and enable scar formation, experimental release of the signalling block led to *gata4* expression and morphological improvement of the injured ventricular wall without loss of scar tissue. Our results indicate that electrically coupled cardiac muscle regenerates after resection injury, primarily through activation and expansion of cardiomyocyte populations. These findings have implications for promoting regeneration of the injured human heart.

After removal of the apex of their cardiac ventricle, zebrafish replace the resected myocardium[4,5]. Although these events involve cardiomyocyte hyperplasia, it is unclear whether proliferating cardiomyocytes derive from existing myocytes or from non-myocyte sources such as stem cells. Identifying cellular contributions to embryonic or regenerative organogenesis has typically involved genetic methods to label different cell types irreversibly and track their progeny[6–11].

While searching for molecular markers informative for regeneration, we identified a unique expression pattern driven by upstream regulatory sequences of *gata4*, a transcription factor gene expressed in the developing embryonic heart and essential for normal cardiac patterning and vascularization[12–17]. Through the use of the *Tg*(*gata4*:*EGFP*)^{ae1} reporter line[18], we found that enhanced green fluorescent protein (EGFP) fluorescence was largely absent in the uninjured adult ventricle. However, after resection of the ventricular apex, *gata4*-driven EGFP was induced in a high percentage of cells throughout the outer compact layer of ventricular myocardium during a period from 3 to 7 days post-amputation (d.p.a.) (Fig. 1a, d, f, g). *gata4*:EGFP was expressed in many cells surrounding and within the injury site by 2 weeks after injury (Fig. 1h), and was limited at all time points to cells positive for myocyte markers (Fig. 1b, c) and negative for markers of the epicardium, a vasculogenic mesothelial layer overlying the compact muscle (Fig. 1e). BrdU (5-bromodeoxyuridine)-labelling studies demonstrated that many *gata4*:EGFP$^+$ cells at the lateral edges of the wound at 7 d.p.a., and within the wound at 14 d.p.a., had recently undergone DNA synthesis (Fig. 1j, k). By 30 d.p.a., a substantial area of the regenerated ventricular wall remained labelled by *gata4*:EGFP fluorescence (Fig. 1i). At these stages, *gata4*:EGFP expression predominantly labelled compact cardiomyocytes, which normally occupy a greater portion of the regenerate than inner trabecular cardiomyocytes[4]. Quantification of fluorescent ventricular muscle at different stages of regeneration by histology indicated progressive redistribution of *gata4*-driven EGFP expression from wound edges into the injury site (Supplementary Fig. 2a, b).

To clarify the dynamics of these events, we generated new transgenic strains to facilitate inducible, Cre-recombinase-based lineage-tracing from *gata4*$^+$ cells. We created a line with a tamoxifen-inducible Cre recombinase–oestrogen receptor fusion protein driven by *gata4* regulatory sequences, *Tg*(*gata4:ERCreER*)^{pd39}, as well as an indicator line that would permit visualization of cardiomyocyte EGFP fluorescence after excision of *loxP*-flanked stop sequences, *Tg*(*bactin2:loxP-DsRed-STOP-loxP-EGFP*)^{s928} (*β-act2:RSG*; Supplementary Fig. 3). We injected 4-hydroxytamoxifen (4-HT) or vehicle once daily into *gata4:ERCreER; β-act2:RSG* animals from 5–7 d.p.a., a time point preceding detectable *gata4*-driven EGFP fluorescence in the injury site. Injection of *gata4:ERCreER; β-act2:RSG* animals with 4-HT, but not vehicle, labelled what presumably represented a subset of myocytes that fluoresced in the *gata4*:EGFP line, revealing a small number of EGFP$^+$ cardiomyocytes bordering the wound by 9 d.p.a. Moreover, contiguous regions of EGFP$^+$ cardiomyocytes could be detected in the injury site by 14 d.p.a. (Fig. 2a), representing a quantifiably significant expansion in labelled cardiac muscle at 20 d.p.a. (Supplementary Fig. 2a, c). These findings indicated a mechanism in which subepicardial cells throughout the ventricle respond to injury by inducing *gata4* expression, with cells near the injury site proliferating and contributing a high proportion of new cardiomyocytes.

Although confocal imaging colocalized *gata4*-driven EGFP and muscle markers, it remained possible that non-myocytes induced *gata4* after injury and rapidly differentiated into proliferative cardiomyocytes. To test the extent to which existing cardiomyocytes

[1]Department of Cell Biology, [2]Howard Hughes Medical Institute, [3]Department of Medicine, Duke University Medical Center, Durham, North Carolina 27710, USA. [4]Cardiovascular Division, Brigham and Women's Hospital, 75 Francis Street, Boston, Massachusetts 02115, USA. [5]Department of Biochemistry and Biophysics, University of California San Francisco, San Francisco, California 94158, USA. [6]Department of Surgery, Weill Cornell Medical College, Cornell University, New York, New York 10021, USA.

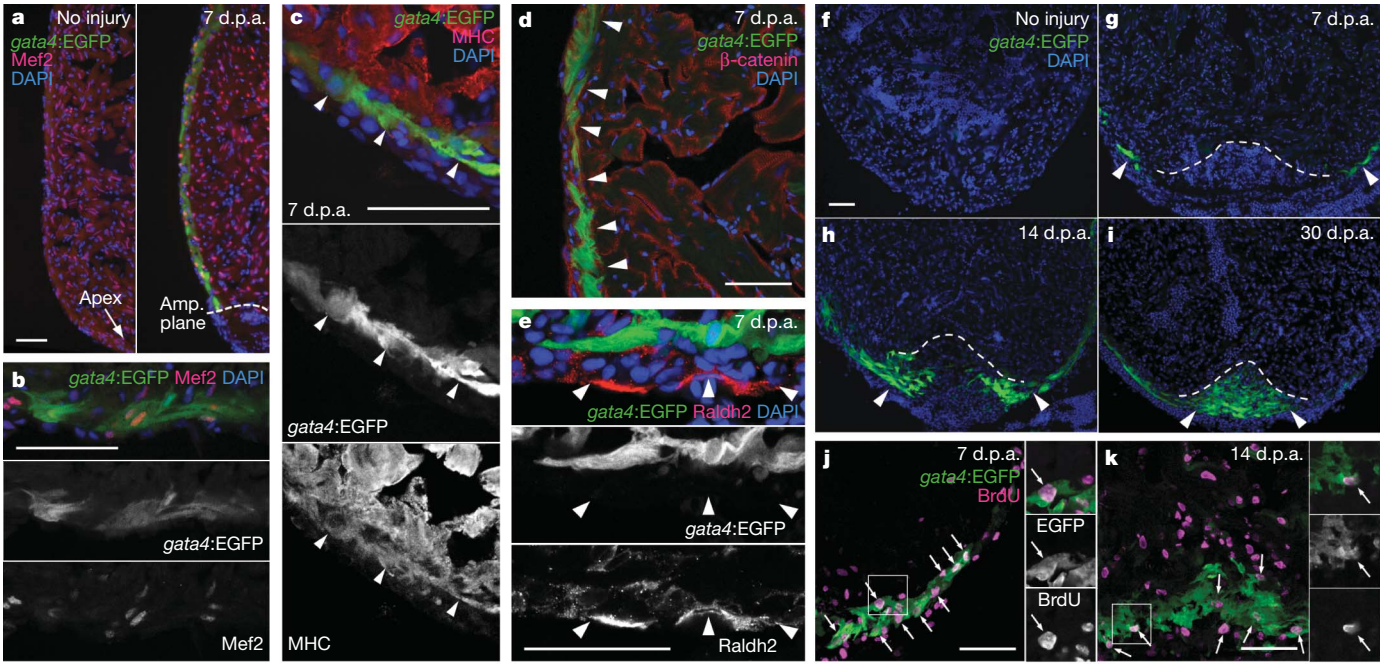

Figure 1 | Cardiomyocytes marked by *gata4*:EGFP are activated by injury and proliferate at the injury site. **a**, *gata4*:EGFP is induced throughout cells in the compact muscle by 7 d.p.a. (right). amp., amputation. **b**, **c**, *gata4*:EGFP (arrowheads in **c**) co-labels with cardiomyocyte markers Mef2 (**b**) and myosin heavy chain (MHC) (**c**). DAPI, 4′,6-diamidino-2-phenylindole. **d**, *gata4*:EGFP (arrowheads) co-stained with β-catenin, indicating EGFP restriction within the myocardial wall. **e**, *gata4*:EGFP does not co-localize with epicardial Raldh2 protein (arrowheads). **f–i**, *gata4*:EGFP expression (arrowheads) in uninjured and regenerating ventricles. Dotted line indicates approximate plane of resection. **j**, **k**, BrdU labelling and immunofluorescence of 7 (**j**) and 14 (**k**) d.p.a. *gata4*:EGFP ventricles. Arrows indicate co-labelling. Single confocal slices are shown in **b**–**e** and insets in **j** and **k**. Confocal projections of 7- or 8-μm *Z*-stacks are shown in **j** and **k**. Scale bars, 50 μm.

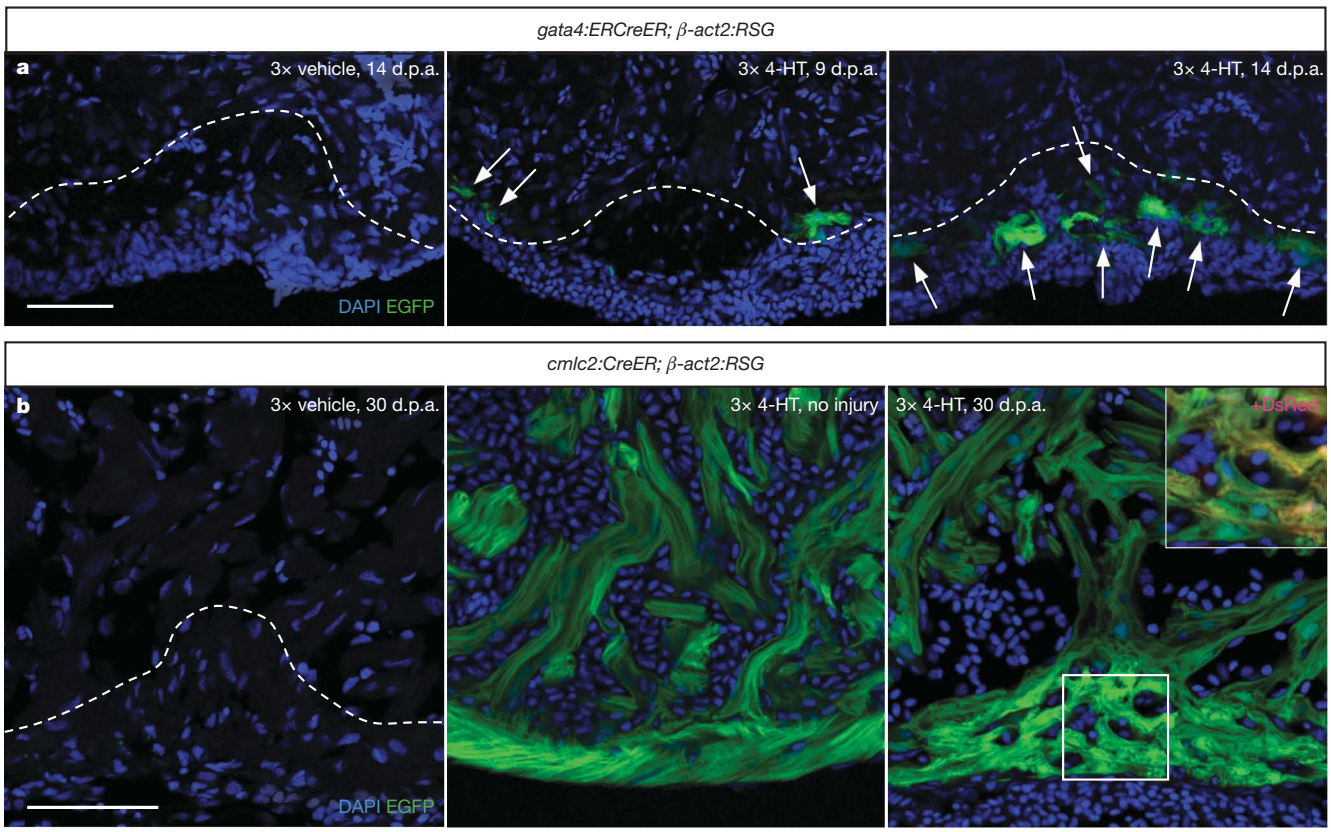

Figure 2 | Major contribution of *gata4*$^+$ cardiomyocytes to heart regeneration. **a**, *gata4:ERCreER; β-act2:RSG* animals injected once daily with vehicle (left) or 4-HT at 5–7 d.p.a., before collection at 9 (centre; $n = 5$) or 14 (right; $n = 6$) d.p.a. EGFP fluorescence (arrows) is observed at injury borders by 9 d.p.a. and within the injury site by 14 d.p.a. Dotted lines denote the approximate plane of resection. **b**, *cmlc2:CreER; β-act2:RSG* animals were injected before injury with vehicle (left) or 4-HT once daily for 3 days. 4-HT labelled the vast majority of cardiomyocytes in uninjured ventricles (centre) and 30 d.p.a. regenerates (right; $n = 10$). Inset, DsRed channel used for calculation of labelling efficiency. Single confocal slices are shown. Scale bars, 50 μm.

contribute to regeneration, we created a strain in which tamoxifen-inducible Cre is driven by regulatory sequences of the contractile gene *cardiac myosin light chain 2* (*cmlc2*, also known as *myl7*), *Tg*(*cmlc2:CreER*)^{pd10}. Measurements of labelling efficiency indicated that our 4-HT-injection protocol tagged ~95% of uninjured *cmlc2:CreER; β-act2:RSG* ventricular cardiomyocytes with EGFP fluorescence (Supplementary Fig. 4). On the basis of analyses of several different indicator lines, labelling by *cmlc2*-driven CreER was specific to cardiomyocytes (Supplementary Fig. 5), and was not instigated by injury or vehicle injection (Fig. 2b). Five days after labelling cardiomyocytes, we resected ventricular apices and allowed 30 days of regeneration. We found no significant difference in the proportion of EGFP$^+$ cardiomyocytes in regenerated *cmlc2:CreER; β-act2:RSG* tissue compared to uninjured ventricles collected 5 or 35 days after injection, a result indicating that the vast majority of new cardiomyocytes derive from cells expressing *cmlc2* before injury (Fig. 2b and Supplementary Fig. 4).

A critical aspect of successful regeneration is the functional incorporation of newly created cells into existing tissue. We labelled whole explanted hearts with the transmembrane-potential-sensitive dye di-4-ANEPPS, and performed optical voltage mapping of surface level cardiomyocytes that include the compact layer and regenerate. At 7 d.p.a., and less-so at 14 d.p.a., there was an increased density of isochrones near the apex of the ventricle as compared to uninjured controls, indicating a marked slowing of conduction (Fig. 3a). Furthermore, electrical activity consistently failed to propagate into the regenerating apex at 7 d.p.a., whereas impulses again conducted throughout the ventricle by 14 d.p.a. when substantial numbers of new *gata4*$^+$ cardiomyocytes appear (Fig. 3a). By 30 d.p.a., isochrone densities at the apex appeared normal (Fig. 3a). These observations were confirmed by direct estimation of conduction velocity, which revealed slowing of distal ventricular conduction at 7 and 14 d.p.a., and normal conduction at 30 d.p.a. (Fig. 3b). We also found evidence of a significant reduction in the maximum depolarization rate at 7 d.p.a., which was fully restored by 14 d.p.a., whereas action potential duration was the same in all groups (Fig. 3c and Supplementary Fig. 6). Thus, our imaging data indicate that electrical coupling of new apical cardiomyocytes begins to occur by ~2 weeks post-injury, with full coupling in the restored wall by 30 d.p.a.

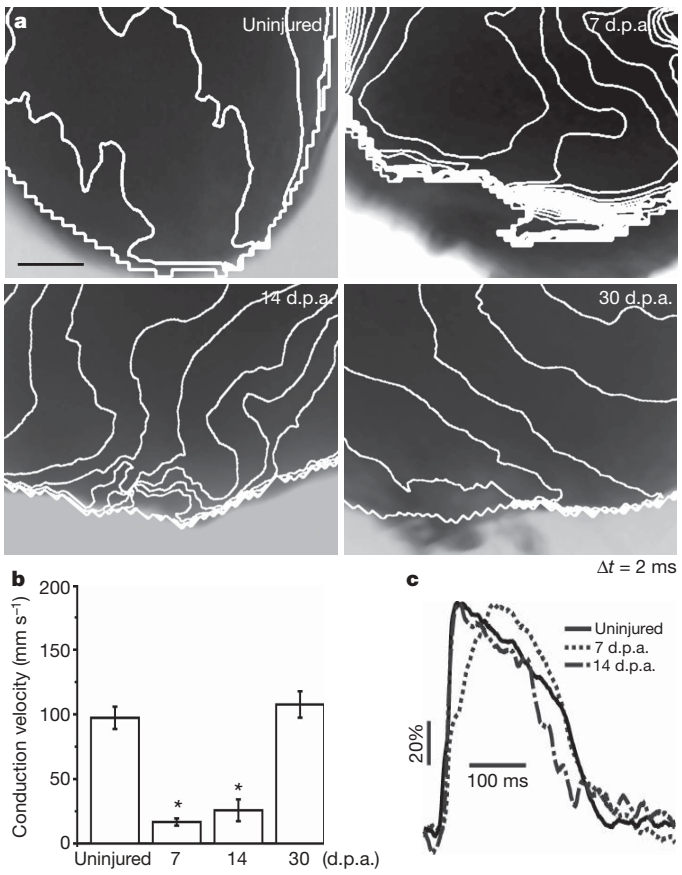

Figure 3 | Electrical coupling of regenerated cardiomyocytes. a, Two-millisecond isochronal density maps of surface myocardium near the apex of explants of uninjured, 7, 14 and 30 d.p.a. ventricles. Scale bar, 100 μm. **b**, Mean conduction velocities measured from local velocity vectors, indicating slowed velocities at 7 and 14 d.p.a. Mean ± s.e.m., $n = 4$–7 ventricles for each time point. *$P < 0.05$ (one-way analysis of variance (ANOVA)). **c**, Representative traces of surface action potentials, indicating a slowing of the maximum depolarization rate at 7 d.p.a.

The normal regenerative response of the zebrafish heart to injury is thought to deter or out-compete a secondary scarring response[4]. To test whether regeneration can occur after a scar is established, we injured *Tg*(*hsp70:dn-fgfr1*)^{pd1} ventricles and induced expression of a dominant-negative fibroblast growth factor (Fgf) receptor by heat-shock for 30 days, causing regenerative arrest and scarring[19] (Fig. 4a, b). Then, we enabled Fgf signalling by removal from heat-shocks for 14 or 60 days. Interestingly, 14 days of restored Fgf signalling increased myocardium in 73% of wounds (Supplementary Fig. 7), with *hsp70:dn-fgfr1; gata4*:EGFP apices containing areas of *gata4*:EGFP$^+$ cardiomyocytes (Fig. 4c, d). When we restored Fgf signalling to scarred hearts for an extended period of 60 days, fibrin was cleared from the wounds, although we did not observe loss of scar tissue. Notably, 90% of injury sites showed histological improvement after extended restoration of Fgf signalling, including 60% that had formed a contiguous wall of muscle enveloping the scar (Fig. 4e–h). These findings suggest that regenerative signals are maintained in zebrafish hearts with established injury scars, an environment that in mammals presents a hurdle for cell-based therapies of myocardial infarction[20,21]. Accordingly, mechanisms that underlie zebrafish heart regeneration might be pertinent to human survivors of myocardial infarction possessing mature scar tissue and compromised ventricular walls.

Earlier studies assessed fast- (EGFP) and slow- (nuclear DsRed2) folding reporters in double transgenic *Tg*(*cmlc2:EGFP*)$^{f1\ or\ twu26}$; *Tg*(*cmlc2:nucDsRed2*)^{f2} zebrafish to document evidence for fresh maturation of *cmlc2*$^-$ progenitor cells into proliferative cardiomyocytes. Specifically, many EGFP$^+$ nucDsRed2$^-$ cardiomyocytes were observed in the developing embryonic heart and the regenerating adult ventricle[19,22]. We re-explored this developmental timing assay by substituting a cytosolic DsRed2 reporter of *cmlc2* that removes the element of nuclear localization that might reduce reporter sensitivity during dynamic developmental events (*Tg*(*cmlc2:DsRed2*)^{pd15}). We observed EGFP$^+$ DsRed2$^-$ myocytes in embryos but not in 7 d.p.a. adult regenerates, which instead contained EGFP$^+$ DsRed2$^+$ myocytes with each cytosolic reporter fluorescing at lower intensities than in non-regenerating muscle (Supplementary Fig. 8). Together with *cmlc2:CreER* lineage-tracing data, these new results argue for modifying the previous interpretation, and indicate that cardiomyocytes participating in regeneration possess or acquire an immature phenotype with reduced *cmlc2* expression. Such a phenotype is possibly reflected by ultrastructural features of cardiomyocytes in 14 d.p.a. regenerates that we did not observe in subepicardial cardiomyocytes of uninjured ventricles, including reduced sarcomeric structure, dysmorphic mitochondria, and low mitochondrial density (Supplementary Fig. 9).

In conclusion, we have identified new mechanistic aspects of zebrafish heart regeneration germane to the origin, function and capabilities of regenerated cardiomyocytes. Foremost, we found that a subpopulation of cardiomyocytes within the ventricular wall activates *gata4* regulatory sequences, proliferates, and contributes substantially to local muscle regeneration. The extent to which other cell populations possibly supply the regenerate awaits further direct lineage-tracing experiments. Notably, the activation of *gata4*:EGFP expression in subepicardial cardiomyocytes parallels the rapid, chamber-wide injury response of the overlying epicardial cells before

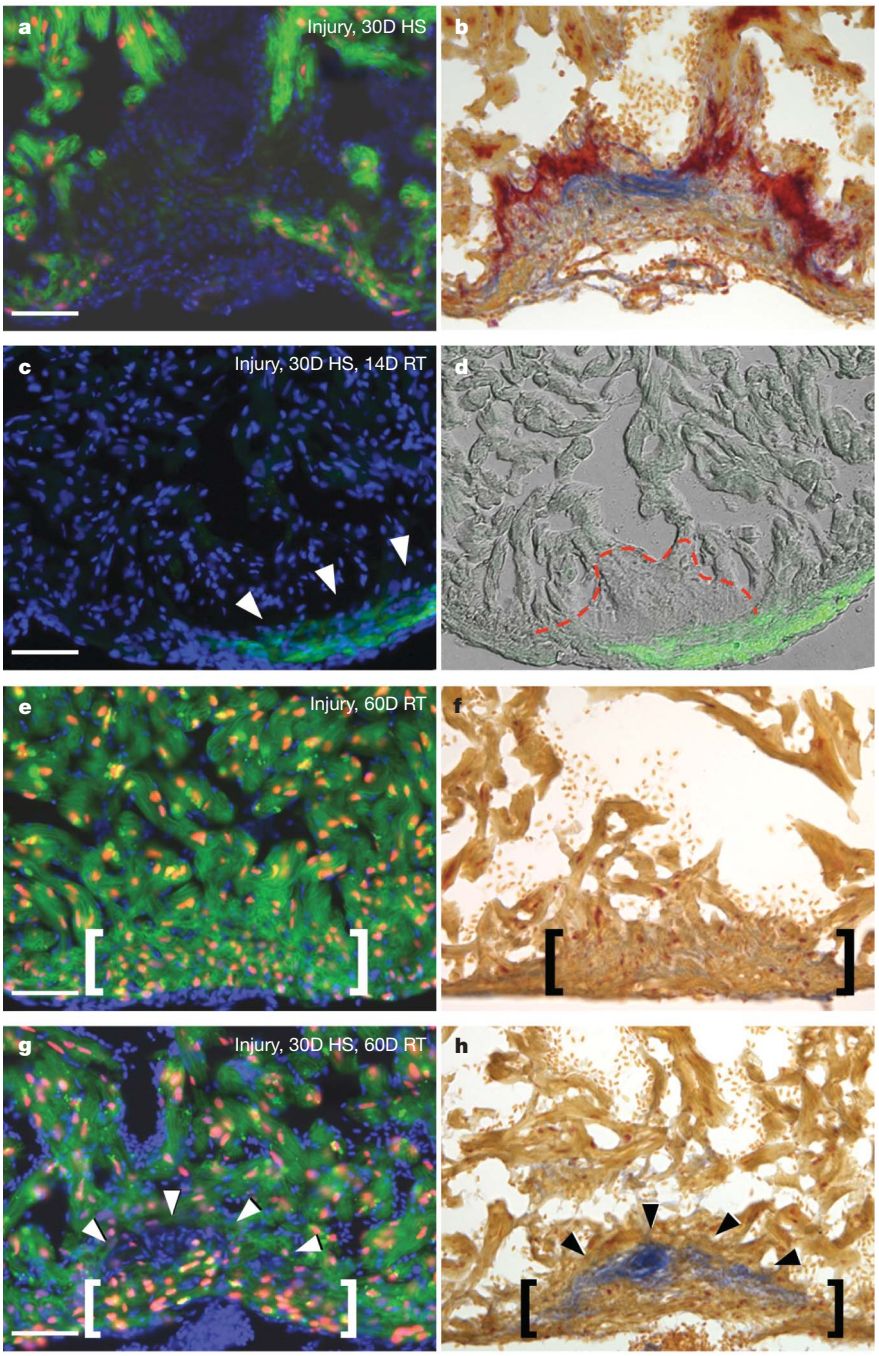

Figure 4 | Restoration of *gata4*:EGFP expression and a new ventricular wall after scarring. **a**, **b**, Typical wound after resection and 30 days (D) Fgf receptor (Fgfr) inhibition. HS, heat-shock. **c**, **d**, *gata4*:EGFP fluorescence (arrowheads) induced by a regimen of injury, 30 days Fgfr inhibition, and 14 days recovery at room temperature (RT; $n = 8$). Dotted line indicates wound. **e**, **f**, Normal regeneration (brackets) after injury and room temperature incubation for 60 days. **g**, **h**, 60 days room-temperature recovery, after resection and 30 days Fgfr inhibition, improves wall anatomy (brackets) without removing scar (arrowheads; $n = 10$). Green, EGFP-tagged Dnfgfr1; red, myocyte nuclei via *cmlc2:nucDsRed2* transgene in **a**, **e** and **g**. Acid fuchsin orange G stain (red, fibrin; blue, collagen) in **b**, **f** and **h**. Animals were heat-shocked 4 h before heart collection in **e** and **g**, inducing EGFP. Scale bars, 50 μm.

they also incorporate into the regenerating area[19]. The similar spatiotemporal dynamics of these muscularizing and vascularizing tissues suggests important interactions as they each become activated, proliferate, and integrate into the injury site.

Our findings are intriguing in light of recent reports describing factors that when introduced can increase proliferation of differentiated cardiomyocytes and improve function in the injured adult mammalian heart[23–26]. It is likely that the zebrafish heart provides an optimized injury environment that encourages activation and/or proliferation of cardiomyocyte subpopulations. Cre-based tools in zebrafish, including those we have described here, will enable precise experimental manipulation of gene expression or function in attempts to modify the injury environment or regenerative response. With knowledge of a key origin of new cardiomyocytes, the cellular and molecular regulatory interactions that mediate heart regeneration in zebrafish can now be more informatively pursued.

METHODS SUMMARY

Outbred Ekkwill strain (EK) or EK/AB mixed background zebrafish 6–12 months of age were used for ventricular resection surgeries as described previously[4]. All transgenic strains were analysed as hemizygotes; details of their construction are described in the Methods. Animal density was maintained at

~4 fish l^{-1} in all experiments. 4-hydroxytamoxifen (4-HT) (Sigma) dissolved in ethanol (5 mg ml^{-1}) was diluted in water to 0.5 mg ml^{-1} for intraperitoneal injections. Ten per cent ethanol was used as a vehicle control. EGFP labelling quantification is described in the Methods. Heat-shock experiments were performed as described previously[27], using double transgenic *hsp70:dnfgfr1; cmlc2:nucDsRed2* or *hsp70:dnfgfr1; gata4*:EGFP animals. For BrdU-incorporation experiments, 2.5 mg ml^{-1} BrdU (Sigma) was injected intraperitoneally once daily for 3 days before collection. Immunofluorescence, *in situ* hybridization, and acid fuchsin orange G stains (detecting fibrin and collagen) were performed as described previously[4]. Primary antibodies used in this study were: anti-Mef2 (rabbit; Santa Cruz Biotechnology), anti-Myosin heavy chain (F59, mouse; Developmental Studies Hybridoma Bank), anti-β-catenin (rabbit; Sigma), anti-zf Raldh2 (rabbit: Abmart), anti-BrdU (rat; Accurate), and anti-GFP (rabbit, used only for co-detection with BrdU; Invitrogen). Secondary antibodies (Invitrogen) used in this study were Alexa Fluor 594 goat anti-rabbit IgG (H+L) for anti-Mef2, Alexa Fluor 594 goat anti-mouse IgG (H+L) for F59, Alexa Fluor 594 goat anti-rat IgG (H+L) for anti-BrdU, and Alexa Fluor 488 goat anti-rabbit IgG (H+L) for anti-GFP. *In situ* hybridization and immunofluorescence images were taken using a Leica DM6000 microscope with a Retiga-EXi camera (Q-IMAGING), and confocal images were taken using a Leica SP2 or SP5 confocal microscope. Physiology methods are described in the Methods.

Full Methods and any associated references are available in the online version of the paper at www.nature.com/nature.

Received 19 August 2009; accepted 7 January 2010.

1. Bergmann, O. *et al.* Evidence for cardiomyocyte renewal in humans. *Science* **324,** 98–102 (2009).
2. Quaini, F. *et al.* Chimerism of the transplanted heart. *N. Engl. J. Med.* **346,** 5–15 (2002).
3. Rubart, M. & Field, L. J. Cardiac regeneration: repopulating the heart. *Annu. Rev. Physiol.* **68,** 29–49 (2006).
4. Poss, K. D., Wilson, L. G. & Keating, M. T. Heart regeneration in zebrafish. *Science* **298,** 2188–2190 (2002).
5. Raya, A. *et al.* Activation of notch signaling pathway precedes heart regeneration in zebrafish. *Proc. Natl Acad. Sci. USA* **100,** 11889–11895 (2003).
6. Cai, C. L. *et al.* Isl1 identifies a cardiac progenitor population that proliferates prior to differentiation and contributes a majority of cells to the heart. *Dev. Cell* **5,** 877–889 (2003).
7. Dor, Y., Brown, J., Martinez, O. I. & Melton, D. A. Adult pancreatic beta-cells are formed by self-duplication rather than stem-cell differentiation. *Nature* **429,** 41–46 (2004).
8. Hsieh, P. C. *et al.* Evidence from a genetic fate-mapping study that stem cells refresh adult mammalian cardiomyocytes after injury. *Nature Med.* **13,** 970–974 (2007).
9. Laugwitz, K. L. *et al.* Postnatal $isl1^{+}$ cardioblasts enter fully differentiated cardiomyocyte lineages. *Nature* **433,** 647–653 (2005).
10. Meilhac, S. M. *et al.* A retrospective clonal analysis of the myocardium reveals two phases of clonal growth in the developing mouse heart. *Development* **130,** 3877–3889 (2003).
11. Zhou, B. *et al.* Epicardial progenitors contribute to the cardiomyocyte lineage in the developing heart. *Nature* **454,** 109–113 (2008).
12. Holtzinger, A. & Evans, T. Gata4 regulates the formation of multiple organs. *Development* **132,** 4005–4014 (2005).
13. Crispino, J. D. *et al.* Proper coronary vascular development and heart morphogenesis depend on interaction of GATA-4 with FOG cofactors. *Genes Dev.* **15,** 839–844 (2001).
14. Molkentin, J. D., Lin, Q., Duncan, S. A. & Olson, E. N. Requirement of the transcription factor GATA4 for heart tube formation and ventral morphogenesis. *Genes Dev.* **11,** 1061–1072 (1997).
15. Kuo, C. T. *et al.* GATA4 transcription factor is required for ventral morphogenesis and heart tube formation. *Genes Dev.* **11,** 1048–1060 (1997).
16. Zeisberg, E. M. *et al.* Morphogenesis of the right ventricle requires myocardial expression of *Gata4*. *J. Clin. Invest.* **115,** 1522–1531 (2005).
17. Pu, W. T., Ishiwata, T., Juraszek, A. L., Ma, Q. & Izumo, S. GATA4 is a dosage-sensitive regulator of cardiac morphogenesis. *Dev. Biol.* **275,** 235–244 (2004).
18. Heicklen-Klein, A. & Evans, T. T-box binding sites are required for activity of a cardiac GATA-4 enhancer. *Dev. Biol.* **267,** 490–504 (2004).
19. Lepilina, A. *et al.* A dynamic epicardial injury response supports progenitor cell activity during zebrafish heart regeneration. *Cell* **127,** 607–619 (2006).
20. Laflamme, M. A., Zbinden, S., Epstein, S. E. & Murry, C. E. Cell-based therapy for myocardial ischemia and infarction: pathophysiological mechanisms. *Annu. Rev. Pathol.* **2,** 307–339 (2007).
21. Passier, R., van Laake, L. W. & Mummery, C. L. Stem-cell-based therapy and lessons from the heart. *Nature* **453,** 322–329 (2008).
22. de Pater, E. *et al.* Distinct phases of cardiomyocyte differentiation regulate growth of the zebrafish heart. *Development* **136,** 1633–1641 (2009).
23. Bersell, K., Arab, S., Haring, B. & Kuhn, B. Neuregulin1/erbb4 signaling induces cardiomyocyte proliferation and repair of heart injury. *Cell* **138,** 257–270 (2009).
24. Kühn, B. *et al.* Periostin induces proliferation of differentiated cardiomyocytes and promotes cardiac repair. *Nature Med.* **13,** 962–969 (2007).
25. Engel, F. B., Hsieh, P. C., Lee, R. T. & Keating, M. T. Fgf1/p38 map kinase inhibitor therapy induces cardiomyocyte mitosis, reduces scarring, and rescues function after myocardial infarction. *Proc. Natl Acad. Sci. USA* **103,** 15546–15551 (2006).
26. Engel, F. B. *et al.* p38 map kinase inhibition enables proliferation of adult mammalian cardiomyocytes. *Genes Dev.* **19,** 1175–1187 (2005).
27. Wills, A. A., Holdway, J. E., Major, R. J. & Poss, K. D. Regulated addition of new myocardial and epicardial cells fosters homeostatic cardiac growth and maintenance in adult zebrafish. *Development* **135,** 183–192 (2008).

Supplementary Information is linked to the online version of the paper at www.nature.com/nature.

Acknowledgements We thank J. Burris and A. Eastes for zebrafish care, X. Meng and the Developmental Studies Hybridoma Bank for antibodies, M. Gignac for help with electron microscopy, laboratory members for comments on the manuscript, and G. Burns, P. Chambon and G. Felsenfeld for plasmids. This work was supported by postdoctoral fellowships from AHA (K.K. and Y.F.), JDRF (R.M.A.), and JSPS (K.K.); NIH training grants HL007208 at Massachusetts General Hospital (A.A.W.) and HL007101 at Duke University Medical Center (G.F.E.); grants from NHLBI (HL064282 to T.E., HL054737 to D.Y.R.S., and HL081674 to K.D.P.), NIGMS (GM075846 to C.A.M.), and March of Dimes (C.A.M.); and grants from AHA, Pew Charitable Trusts and Whitehead Foundation (K.D.P.).

Author Contributions K.K. and K.D.P. designed experimental strategy, analysed data, and prepared the manuscript. K.K., J.E.H. and Y.F. generated and characterized transgenic lines for lineage-tracing. R.M.A. and D.Y.R.S. provided unpublished reagents for lineage-tracing. K.K., J.E.H. and K.D.P. performed regeneration experiments. J.E.H. performed electron microscopy. A.A.W., G.F.E. and C.A.M. designed physiology experiments and interpreted data. A.A.W. performed optical mapping assays. T.E. helped design strategy and provided key reagents. All authors commented on the manuscript.

Author Information Reprints and permissions information is available at www.nature.com/reprints. The authors declare no competing financial interests. Correspondence and requests for materials should be addressed to K.D.P. (k.poss@cellbio.duke.edu).

METHODS

Construction of *gata4:ERCreER* transgenic animals. ER^{T2}-Cre-ER^{T2} complementary DNA from pCAG-ERT2CreERT2 (ref. 28) was cloned downstream of the 14.8-kilobase (kb) *gata4* promoter[18]. The entire construct was flanked with I-SceI sites for transgenesis using the meganuclease method[29]. The full name of this transgenic line is *Tg*(*gata4:ERCreER*)^{pd39}.

Construction of *cmlc2:CreER* transgenic animals. Cre-ER^{T2} cDNA from pCre-ERT2 (ref. 30) was cloned downstream of the 5.1-kb *cmlc2* promoter[31]. A DsRed-Ex cassette controlled by the lens-specific *crystallin, alpha A* promoter was also included (*cryaa:DsRed*), which enables visual identification of transgenic animals by lens fluorescence[32], and was subcloned upstream of the *cmlc2:CreER* sequences in the opposite orientation. The entire construct was flanked with two copies of the core element of the chicken β-globin insulator (2× core insulator elements) (provided by G. Felsenfeld), and then flanked with I-SceI sites. The full name of this transgenic line is *Tg*(*cmlc2:CreER*)^{pd10}.

Construction of *β-act2:RSG* transgenic animals. We subcloned 9.8 kb of genomic DNA immediately upstream of the *bactin2* transcriptional start site into a modified pBSK vector with a multiple cloning site flanked by I-SceI restriction sites. A *loxP-DsRed-STOP-loxP-EGFP* cassette was then subcloned downstream of the *bactin2* promoter. The DsRed-STOP cassette serves as a marker for the transgene, and also prevents read-through translation of EGFP protein. This construct was injected into one-cell-stage wild-type embryos using standard meganuclease transgenesis techniques[29]. One founder was isolated and propagated from the injected embryos. The full name of this transgenic line is *Tg*(*bactin2:loxP-DsRed-STOP-loxP-EGFP*)^{s928}.

Construction of 5-kb *β-act2:RnG* and *hsp70:RnG* transgenic animals. The pBigT vector was used to make a cassette containing a floxed mCherry cassette with a transcriptional stop, upstream of an EGFP cassette tagged with three copies of nuclear localization signals (3× NLS-EGFP) downstream of the second *loxP* site. The resulting cassette (*loxP-mCherry-STOP-loxP-nucEGFP*) was then subcloned downstream of a ~5.3-kb fragment of the ~10-kb zebrafish *bactin2* promoter, or a ~1.5-kb zebrafish *hsp70* promoter. The constructs were flanked with two copies of the core element of the chicken globin insulator (2× core insulator elements) (provided by G. Felsenfeld), as well as two I-SceI sites. The full names of the transgenic lines are *Tg*(*bactin2:loxP-mCherry-STOP-loxP-nucEGFP*)^{pd31} and *Tg*(*hsp70l:loxP-mCherry-STOP-loxP-nucEGFP*)^{pd30}.

Construction of *gata5:RnG* transgenic animals. The translational start codon of *gata5* in the BAC clone DKEYP-73A2 was replaced with the *loxP-mCherry-STOP-loxP-nucEGFP* (RnG) cassette by Red/ET recombineering technology (GeneBridges). The 5′ and 3′ homologous arms for recombination were a 716-base-pair (bp) fragment upstream of the start codon, and a 517-bp fragment downstream, respectively, and were subcloned to flank the RnG cassette. To avoid potential mis-recombination between the RnG cassette and an endogenous *loxP* site in the BAC vector, we replaced the vector-derived *loxP* site with an I-SceI site using the same technology. The final BAC was purified with nucleobond BAC 100 kit (Clontech), and co-injected with meganuclease into one-cell-stage zebrafish embryos. The full name of this transgenic line is *Tg*(*gata5:loxP-mCherry-STOP-loxP-nucEGFP*)^{pd40}.

Construction of *cmlc2:DsRed2* transgenic animals. DsRed2 cDNA was cloned behind the 5.1-kb *cmlc2* promoter, and the entire cassette was flanked with I-SceI sites. The full name of this transgenic line is *Tg*(*cmlc2:DsRed2*)^{pd15}.

4-HT labelling and quantification of EGFP fluorescence in *cmlc2:CreER; β-act2:RSG* animals. To determine the kinetics of 4-HT labelling, we gave single 20 μl intraperitoneal injections of a low dose (2.5 μg ml^{-1}) of 4-HT to uninjured *cmlc2:CreER; β-act2:RSG* adults. We detected recombination by myocyte EGFP fluorescence in ventricular sections at 1 day post-injection (d.p.i.), and at increased frequency (~20% of ventricular myocytes) and intensity by 2 d.p.i. Examination of ventricular sections at 3, 4 and 5 days after injection indicated EGFP labelling frequencies similar to 2 d.p.i. These findings provided evidence that intraperitoneally injected 4-HT is no longer able to stimulate new recombination events in ventricular cardiomyocytes of adult zebrafish after 2 d.p.i.

To quantify Cre-mediated release of EGFP expression in lineage tracing experiments with *cmlc2:CreER; β-act2:RSG* animals, three sections including the regenerate were selected from each heart. For uninjured control hearts, the three largest sections were selected from each heart as described previously[27]. We used the $DsRed^+$ area to reflect total myocardial section surface area, as the background expression of DsRed persists in cardiac muscle after 4-HT injections in *β-act2:RSG* transgenic fish. This is probably due to multiple transgene copies, allowing escape of some floxed DsRed cassettes from Cre-mediated recombination (Supplementary Fig. 2). Images of single optical slices of the ventricular apex were taken at ×40 (1,024 × 1,024 pixels) by adjusting gain to detect EGFP or DsRed signals above the background level. An area (504 × 504 pixels) at the injured apex was chosen to include most of the regenerate in the image, and cropped using Photoshop software. An identical area was cropped at the ventricular apex for uninjured animals. $EGFP^+$ and $DsRed^+$ areas were quantified in pixels by ImageJ software, and the percentage of $EGFP^+$ versus $DsRed^+$ areas was calculated.

Quantification of EGFP fluorescence in *gata4*:EGFP and *gata4:ERCreER; β-act2:RSG* animals. To quantify $EGFP^+$ areas, three sections including the wound/regenerate were selected from each heart. Images of the ventricular apex were taken at ×20 using a Leica DM6000 microscope with a Retiga-EXi camera (Q-IMAGING). An area (109 × 109 pixels for *gata4*:EGFP animals and 73 × 73 pixels for *gata4:ERCreER; β-act2:RSG* animals) was designated at each of the lateral wound edges and cropped using Photoshop software (see Supplementary Fig. 2 for cartoon). An area (109 × 218 pixels for *gata4*:EGFP animals and 73 × 146 pixels for *gata4:ERCreER; β-act2:RSG* animals) non-overlapping with the lateral areas was designated and cropped at the injury site. $EGFP^+$ areas were quantified in pixels by ImageJ software, and the number of pixels summed and averaged to yield an edge $EGFP^+$ area and injury site $EGFP^+$ area for each heart.

Transmission electron microscopy. Injured hearts were fixed in 2.5% glutaraldehyde, 2% formaldehyde in 0.1 M sodium cacodylate buffer. Tissue was post-fixed in 1% OsO4, dehydrated, embedded in Spurr's resin (EMS), and sectioned to 70–90 nm thickness using Ultracut or Ultracut E ultra-microtomes (Leica). The sections were counterstained with uranyl acetate and lead citrate. Microscopy was performed on a FEI Tecnai G2 Twin transmission electron microscope and images were obtained using a Hamamatsu ORCA-HR digital camera and AMT software.

Optical mapping. Fish were anaesthetized with 0.1% 3-aminobenzoic acid methyl ester, and hearts were isolated within 30 s and placed in Tyrode solution containing (in mM) Na^+ (136), K^+ (5.4), Mg^{2+} (1.0), PO_4^{3-} (0.3), Ca^{2+} (1.8), glucose (5.0) and HEPES (10.0) at pH 7.4. Hearts were loaded for 10 min with the transmembrane-potential-sensitive dye di-4-ANEPPS (D-1199, Invitrogen), which was dissolved in Tyrode solution. After staining, the preparations were transferred into the recording chamber (Warner Instruments), which contained Tyrode solution supplemented with 30 μM of the excitation-contraction decoupler blebbistatin (EMD Chemicals) to inhibit contraction during optical measurements. The chamber was mounted onto the stage of an inverted microscope (TE-2000U, Nikon) equipped with a high-speed CCD camera (Cardio CCD-SMQ, Redshirt Imaging) with an 80 × 80 pixel frame. Hearts were point-stimulated at 60 beats-per-minute using a fine platinum electrode held in place near the base of the heart using a micro-manipulator. This electrode location eliminated artefactual increases in conduction velocity due to simultaneous local capture of multiple pixels proximate to the stimulus site (that is, virtual electrode effects)[33]. Optical action potentials were recorded from the epicardial surface of the apex. Fluorescence was excited with a 120 W metal-halide arc lamp (X-Cite 122, Exfo) and filtered at 540 ± 25 nm. Fluorescence emission was passed through a long-pass emission filter (585 nm) before being focused onto the camera. Optical magnification was ×2 resulting in 11-μm spatial resolution between recording pixels. The camera was operated at 2,000 frames-per-second and signals were digitized with 14-bit precision. Signals were digitally filtered in the temporal (900 Hz cutoff) and spatial (4-pixel weighted average) domains to reduce noise. Action potentials recorded with this system depicted the time course of membrane potential change with fidelity comparable to action potentials recorded with patch-clamp technique[34].

Optical mapping fluorescence data analysis. Acquired fluorescence data were analysed using custom software written specifically for the analysis of action potentials recorded optically from the zebrafish heart (MatLab, Mathworks). Action potential duration (APD) was defined as the time interval between 20% depolarization and 80% return or repolarization to resting potential (APD_{80}). Action potential upstroke velocity was derived from the maximum of the first time-derivative of the action potential. Activation time was defined as the time of 50% depolarization during the rising phase of the action potential. We have used this criterion of local activation because the time at half-maximum depolarization has been shown previously in computer simulations to correspond closely to the maximum cellular sodium influx[35]. Isochronal maps that display the position of the wavefront at constant time intervals (2 ms) were constructed from the activation times using the contour plotting functions provided by the Matlab software. Conduction velocity vector fields were estimated from the activation times using an established algorithm described previously[36]. In brief, local velocity vectors, which represent the magnitude and direction of the propagating depolarizing wave at each recording site, were calculated by fitting the depolarization time measured at each site to a parabolic two-dimensional surface. The components of the velocity vector at each site were calculated from the components of the gradient on this surface. Conduction velocities were averaged across sites located within a 200 × 200 μm square near the apex of each heart (Supplementary Fig. 10).

28. Matsuda, T. & Cepko, C. L. Controlled expression of transgenes introduced by *in vivo* electroporation. *Proc. Natl Acad. Sci. USA* **104**, 1027–1032 (2007).

29. Thermes, V. *et al.* I-scei meganuclease mediates highly efficient transgenesis in fish. *Mech. Dev.* **118,** 91–98 (2002).
30. Indra, A. K. *et al.* Temporally-controlled site-specific mutagenesis in the basal layer of the epidermis: comparison of the recombinase activity of the tamoxifen-inducible Cre-ER(T) and Cre-Er(T2) recombinases. *Nucleic Acids Res.* **27,** 4324–4327 (1999).
31. Rottbauer, W. *et al.* Reptin and pontin antagonistically regulate heart growth in zebrafish embryos. *Cell* **111,** 661–672 (2002).
32. Waxman, J. S., Keegan, B. R., Roberts, R. W., Poss, K. D. & Yelon, D. Hoxb5b acts downstream of retinoic acid signaling in the forelimb field to restrict heart field potential in zebrafish. *Dev. Cell* **15,** 923–934 (2008).
33. Sidorov, V. Y., Holcomb, M. R., Woods, M. C., Gray, R. A. & Wikswo, J. P. Effects of unipolar stimulation on voltage and calcium distributions in the isolated rabbit heart. *Basic Res. Cardiol.* **103,** 537–551 (2008).
34. Brette, F. *et al.* Characterization of isolated ventricular myocytes from adult zebrafish (*Danio Rerio*). *Biochem. Biophys. Res. Commun.* **374,** 143–146 (2008).
35. Fast, V. G. & Kleber, A. G. Cardiac tissue geometry as a determinant of unidirectional conduction block: assessment of microscopic excitation spread by optical mapping in patterned cell cultures and in a computer model. *Cardiovasc. Res.* **29,** 697–707 (1995).
36. Bayly, P. V. *et al.* Estimation of conduction velocity vector fields from epicardial mapping data. *IEEE Trans. Biomed. Eng.* **45,** 563–571 (1998).